

DOI: <https://doi.org/10.17816/vto253610>

# Characteristics of *m. Psoas minor* and *m. Sacrocaudalis (coccygeus) dorsalis lateralis* in simultaneous modeling of lateral interbodial spinnylodesis and posterior sacro-iliac joint arthodesis

Galina N. Filimonova<sup>1</sup>, Olga V. Diuriagina<sup>1</sup>, Nikolai I. Antonov<sup>1</sup>, Maksim V. Stogov<sup>1</sup>, Sergei O. Ryabykh<sup>2</sup>, Natalia V. Tushina<sup>1</sup>

<sup>1</sup> Ilizarov National Medical Research Center of Traumatology and Orthopedics, Kurgan, Russia

<sup>2</sup> Priorov National Medical Research Center of Traumatology and Orthopedics, Moscow, Russia

## ABSTRACT

**BACKGROUND:** Simultaneous surgical interventions on the spine with the use of high-tech instruments and minimally invasive access techniques allow to eliminate several problems all at once, to activate patients at an early date and to reduce the number of complications.

**AIM:** To evaluate morphological changes to evaluate morphological changes in the *m. Psoas minor* and *m. Sacrocaudalis dorsalis lateralis* during simultaneous modeling of lateral interbody fusion and posterior sacroiliac joint arthodesis

**MATERIALS AND METHODS:** Experiments were carried out on 14 outbred dogs; 3 animals formed a control group. The animals underwent consecutive lateral interbody fusion of the lumbar spine and posterior arthodesis of the sacroiliac joint. The lumbar spine and sacroiliac joint were stabilized with external fixation device. Paraffin sections of muscles were stained with hematoxylin-eosin, according to Van Gieson, and Masson. Biochemical analysis of blood serum was performed during the experiment.

**RESULTS:** The morphological study of the muscles revealed pathohistological features such as an increase in the variety of myosymplast diameters, loss of their profiles polygonality, massive fibers fatty degeneration, endo- and perimysial fibrosis, sclerotization of vessel membranes, obliteration of their lumens. At the end of the experiment, the degree of the small lumbar muscle fibrosis was 161% and of the sacrocaudal dorsal lateral muscle fibrosis was 240% of the control parameters ( $p < 0.05$ ); the rate of the muscle fatty infiltration was 339 and 310% of the normal value, respectively. The sacroiliac-caudal dorsal lateral muscle underwent more marked changes, especially in the early stages of the experiment. A significant increase in the enzymes activity, skeletal muscle damage markers was detected on the 14th day after surgery.

**CONCLUSION:** Simultaneous surgical interventions on the spine should minimize mechanical effects on the paravertebral muscles and use techniques to stimulate their function in the postoperative period, which will reduce the processes of fibrogenesis and fat involution as well as provide an overall shorter rehabilitation period for the target patients.

**Keywords:** simultaneous operations; lateral interbody fusion; posterior arthodesis; psoas minor; sacrocaudalis dorsalis lateralis muscle; blood biochemistry.

## To cite this article:

Filimonova GN, Diuriagina OV, Antonov NI, Stogov MV, Ryabykh SO, Tushina NV. Characteristics of *m. Psoas minor* and *m. Sacrocaudalis (coccygeus) dorsalis lateralis* in simultaneous modeling of lateral interbodial spinnylodesis and posterior sacro-iliac joint arthodesis. *N.N. Priorov Journal of Traumatology and Orthopedics*. 2022;29(4):379–390. DOI: <https://doi.org/10.17816/vto253610>

Received: 20.02.2023

Accepted: 06.03.2023

Published: 16.03.2023

DOI: <https://doi.org/10.17816/vto253610>

# Характеристика *m. Psoas minor* и *m. Sacrocaudalis (coccygeus) dorsalis lateralis* при симультанном моделировании бокового межтелового спондилодеза и заднего артродеза крестцово-подвздошного сустава

Г.Н. Филимонова<sup>1</sup>, О.В. Дюрягина<sup>1</sup>, Н.И. Антонов<sup>1</sup>, М.В. Стогов<sup>1</sup>, С.О. Рябых<sup>2</sup>, Н.В. Тушина<sup>1</sup><sup>1</sup> НМИЦ травматологии и ортопедии им. акад. Г.А. Илизарова, Курган, Российская Федерация<sup>2</sup> НМИЦ травматологии и ортопедии им. Н.Н. Приорова, Москва, Российская Федерация

## АННОТАЦИЯ

**Введение.** Симультанные хирургические вмешательства на позвоночнике с применением высокотехнологичного инструментария и малоинвазивных методик доступа позволяют одновременно устранить несколько проблем, активизировать пациентов в ранние сроки и уменьшить количество осложнений.

**Цель.** Оценка морфологических изменений малой поясничной и крестцово-каудальной (копчиковой) дорсальной латеральной мышц при симультанном моделировании бокового межтелового спондилодеза и заднего артродеза крестцово-подвздошного сустава.

**Материалы и методы.** Проведены эксперименты на 14 беспородных собаках, 3 особи составили группу контроля. Животным последовательно выполняли боковой межтеловой спондилодез поясничного отдела позвоночника и задний артродез крестцово-подвздошного сустава. Поясничный отдел и крестцово-подвздошный сустав стабилизировали аппаратом внешней фиксации. Парафиновые срезы мышц окрашивали гематоксилином-эозином, по Ван-Гизону, по Массону. На сроках эксперимента проводили биохимический анализ сыворотки крови.

**Результаты.** В ходе морфологического исследования мышц выявлены патогистологические особенности, такие как увеличение разнообразия диаметров миосимпластов, утрата полигональности их профилей, массовая жировая дегенерация волокон, фибрирование эндо- и перимизия, склеротизация оболочек сосудов, облитерация их просветов. По окончании эксперимента степень фиброза малой поясничной мышцы составила 161%, крестцово-каудальной дорсальной латеральной мышцы — 240% от контрольного значения ( $p < 0,05$ ); показатель жировой инфильтрации мышц составил соответственно 339 и 310% от нормы. Более выраженным изменениям подвергается крестцово-каудальная дорсальная латеральная мышца, особенно на ранних этапах эксперимента. Обнаружен достоверно значимый рост активности ферментов — маркеров повреждения скелетных мышц на 14-е сутки после операции.

**Заключение.** При симультанных хирургических вмешательствах на позвоночнике необходимо минимизировать механические воздействия на паравертебральные мышцы, использовать приёмы стимуляции их функции в послеоперационный период, что позволит уменьшить процессы фиброгенеза и жировой инволюции и обеспечит в целом сокращение периода реабилитации целевых пациентов.

**Ключевые слова:** симультанные операции; боковой межтеловой спондилодез; задний артродез; малая поясничная мышца; крестцово-каудальная дорсальная латеральная мышца; биохимия крови.

## Как цитировать:

Филимонова Г.Н., Дюрягина О.В., Антонов Н.И., Стогов М.В., Рябых С.О., Тушина Н.В. Характеристика *m. Psoas minor* и *m. Sacrocaudalis (coccygeus) dorsalis lateralis* при симультанном моделировании бокового межтелового спондилодеза и заднего артродеза крестцово-подвздошного сустава // Вестник травматологии и ортопедии им. Н.Н. Приорова. 2022. Т. 29, № 4. С. 379–390. DOI: <https://doi.org/10.17816/vto253610>

## INTRODUCTION

Simultaneous (combined) surgeries involved up to five different manipulations performed during a single surgical procedure. For example, for polytrauma (with fewer anesthesia procedures), the duration of treatment and recovery is shortened, and the overall stress level of the patient is reduced [1–3]. Combined spinal surgery using high-tech instruments and minimally invasive access techniques allows for dealing with several problems simultaneously, making patients active at an early stage and reducing complications [4]. In severe high-energy injuries of the thoracolumbar spine, combined surgery is a reliable method of achieving sufficient decompression, repositioning, and reconstruction [5]. Multilevel vertebroplasty for multiple compression fractures is also safe and offers significant benefits when performed simultaneously [6].

For degenerative scoliosis of the lumbar spine, the lumbar lateral interbody fusion (LLIF) approach is used [7]. The safety and efficiency of the sacroiliac joint (SIJ) arthrodesis technique with titanium implants for the treatment of degenerative sacroiliitis and joint rupture was established [8]. Triangular titanium implants are increasingly being used for SIJ arthrodesis, resulting in rapid pain reduction and improved quality of life [9–11]. Thus, good results are obtained in minimally invasive arthrodesis with the use of three-dimensional cages (*iFuse Implant System*) [12, 13].

Numerous studies have evaluated paravertebral muscles in spinal pathologies and their status after surgical interventions [14–16]. Microscopic features of muscle tissue, such as myosinplastic diameters, their distribution and profile features, muscle fat infiltration, degree of fibrosis, and muscle atrophy have been evaluated [17, 18]. No studies have examined histological features of paravertebral muscles during concomitant spine surgeries using the LLIF and posterior SIJ arthrodesis, which determined the expediency of this study.

This study aimed to assess morphological changes in the small lumbar (*m. psoas minor*) and sacrococcygeal (coccygeal) dorsal lateral muscles (*m. sacrocaudalis dorsalis lateralis*) during simultaneous simulation of lateral interbody fusion and posterior SIJ arthrodesis.

## MATERIALS AND METHODS

### Study design

The study was conducted at the Ilizarov National Medical Research Center for Traumatology and Orthopedics. It is part of a prospective experimental study on skeletally mature male and female outbred dogs with a bodyweight

of  $13.0 \pm 4.0$  kg and a shin length of 12–14 cm. The level of evidence was IIb.

The experiment was performed in 2019–2021 within the state assignment “Development and assessment of the efficiency of patient-centered implants in the surgery of the axial skeleton,” Direction No. 8. Research registration no. AAAA-A18-118011190118-8. Data processing was conducted in 2022.

### Study ethics

The study was approved by the local ethics committee of the Ilizarov National Medical Research Center for Traumatology and Orthopedics (Minutes No. 2/5 dated May 17, 2018). The animals were kept in aviaries under standard vivarium conditions in accordance with GOST 33215-2014 dated December 22, 2014, No. 73-P “Guidelines for the maintenance and care of laboratory animals: Environment, housing, and management” and GOST 33217-2014 “Guidelines for the maintenance and care of laboratory animals. Species-specific provisions for laboratory predatory mammals.”

### Description of the experimental intervention

The main goal of the experiment was to examine the safety and primary efficiency of 3D titanium cages for interbody fusion and iliosacral blocking. The experimental group consisted of 14 animals, and the control group included three animals. Premedications included 1% dimedrol (0.02 mg/kg), 0.1% atropine sulfate (0.02 mg/kg), 1% droperidol (0.5 mg/kg), and 2% rometar (1 mg/kg). For intravenous anesthesia, 5% sodium thiopental solution at a dose of 10 mg/kg was administered. The animals were removed from the experiment after 6 ( $n=5$ ), 12 ( $n=6$ ), and 18 ( $n=3$ ) months. Euthanasia was performed after premedication, followed by the administration of a lethal dose of barbiturates.

### Experimental model

Surgical access to the lumbar spine was performed on the right side at the level of the apices of the transverse processes of  $L_{IV-VI}$ . The cage was inserted using the impaction method until full penetration into the interbody space (Fig. 1a). The wound was sutured in layers [19]. At the second stage of surgery, sacrocaudal dorsal lateral muscles were displaced medially to access the SIJ at the  $L_{VII}$  and  $S_{I-II}$  levels. A bed for the cage was formed in the articular SIJ surfaces. The adjacent bone tissue of the iliac wing and sacrum was captured. The implant was impacted (Fig. 1b), and the wound was sutured in layers. The SIJ and lumbar spine were stabilized with an Ilizarov apparatus for 30 days.

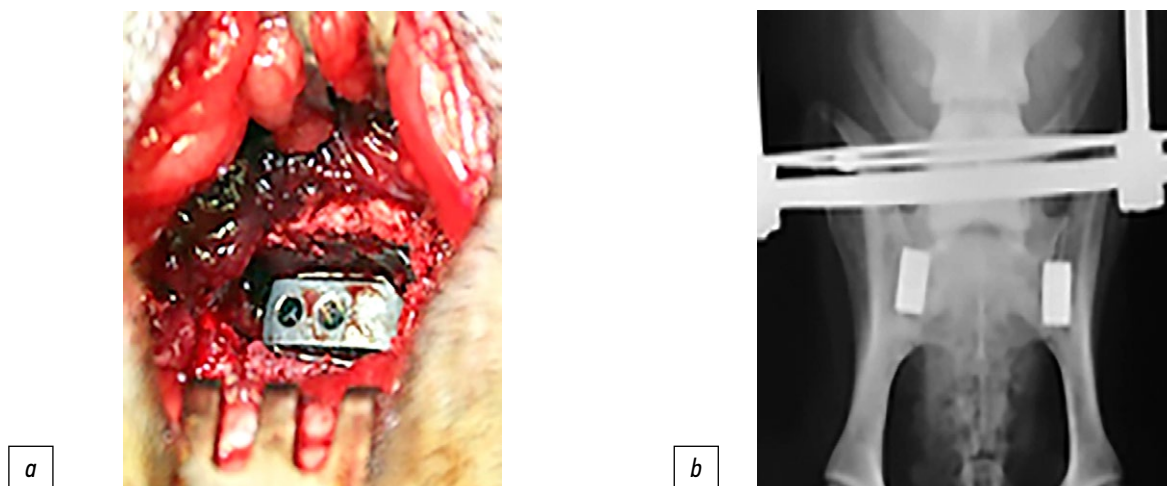


**Fig 1.** Surgical field: *a* — titanium cage between the sacrum and the wings of the ilium of the lumbar vertebrae; *b* — the position of the cages in the sacroiliac joints (sacrum).

### Histological examinations of the paraspinal muscles

The small lumbar and sacrocaudal (coccygeal) dorsal lateral muscles were examined after 6, 12, and 18 months of the experiment. Muscle fragments were excised from the right side of the spine in the projection of implant insertion into the interbody space and fixed in 2% glutaric and 2% paraformaldehyde mixture in equal volumes. After histological examination, the material was embedded in paraffin, and the sections were stained with hematoxylin-eosin according to Van Gieson and Masson trichrome procedures. The sections were examined using an AxioScope. A1 stereomicroscope and an AxioCam digital camera (Carl Zeiss MicroImaging GmbH, Germany). The images were used for stereometry. The volume density ( $\text{mm}^3/\text{mm}^3$ ) of muscle fibers ( $V_{\text{mf}}$ ), microvessels ( $V_{\text{mv}}$ ), endomysium ( $V_{\text{end}}$ ), and nuclear component of the muscle tissue ( $V_{\text{n}}$ ) and the numerical density ( $\text{mm}^{-2}$ ) of the myosmyplasts and microvessels ( $N_{\text{Amf}}$ ,  $N_{\text{Amv}}$ ) were calculated. In addition, the muscle vascularization index ( $I_{\text{vasc}}$ ), which indirectly evaluates muscle oxygenation, was calculated, and  $N_{\text{Amv}}/N_{\text{Amf}}$  was a species constant.

### Biochemical blood serum tests

The serum concentrations of total protein, C-reactive protein, and skeletal muscle damage markers such as creatine phosphokinase (CPK) and aminotransferases (aspartate transaminase and alanine transaminase) were determined at different periods of the experiment. The levels of total protein, C-reactive protein, and enzyme activity were determined on a Hitachi 902 Biochemical Automatic Analyzer (USA) using reagent kits from BioSystem (Spain) and Vector Best (Novosibirsk, Russia).

### Statistical analysis

*Principles of sample size calculation: The sample size was not preliminarily calculated.*

*Methods of statistical data analysis*

1. Static analysis of stereometric data: (a) Digital material was processed using AtteStat version 13.1 (Russia) [20]. (b) Arithmetic mean (M) and standard error of mean (m) were determined. (c) The reliability of differences was estimated using nonparametric Wilcoxon test for independent samples, and the statistical significance level of differences was set at  $p < 0.05$ .
2. Statistical analysis of biochemical data: (a) Digital material was processed using AtteStat version 13.1 (Russia) [20]. (b) The reliability of differences between the values obtained during the experiment was compared with those obtained before the surgery (day 0). (c) Differences were assessed using the Wilcoxon test for dependent samples. Results were presented as median and first and third quartiles.

## RESULTS

In the control group, the histostructures of small lumbar and sacrocaudal (coccygeal) dorsal lateral muscles were characterized by polygonal uniform profiles of muscle fibers, minimal connective tissue interlayers (Fig. 2a), and perimyseal arterial vessels with open lumen and circular orientation of smooth muscle cells (SMCs), without membrane fibrosis (Fig. 2b). Few myosmyplasts with signs of reversible contractures, intramuscular nerve trunks, and neuromuscular spindles of normal structure were observed.

At month 6 of the experiment, both muscles were characterized by signs of structural adaptation to the experimental conditions, such as loss of polygonality of myocyte profiles, increased variability of their diameters, single adipocytes, small groups in the interstitial space, bundles of muscle fibers, and fibrosis of the endomysium and perimysium (Fig. 3a, 3c). In arterial vessels with a significantly thickened medial tunic, in which the SMCs were chaotically oriented, the adventitial tunic was strongly fibrotic, and the lumen was frequently obliterated (Fig. 3b).

After 12 months, the polygonal profiles of myosymplasts prevailed in the histostructure of the small lumbar muscle, and the intramuscular nerve guides and neuromuscular spindles were characteristically normalized (Fig. 4a). In the sacrocaudal dorsal lateral muscle, the above signs of structural adaptation were preserved: symplastic diameters varied, internal nuclei were observed, and inflammatory cells could be found in areas of significant interstitial fibrosis (Fig. 4b). Moreover, muscle fiber bundles were replaced by adipocytes, and perimysial vessels had signs of adventitial fibrosis (Fig. 4c).

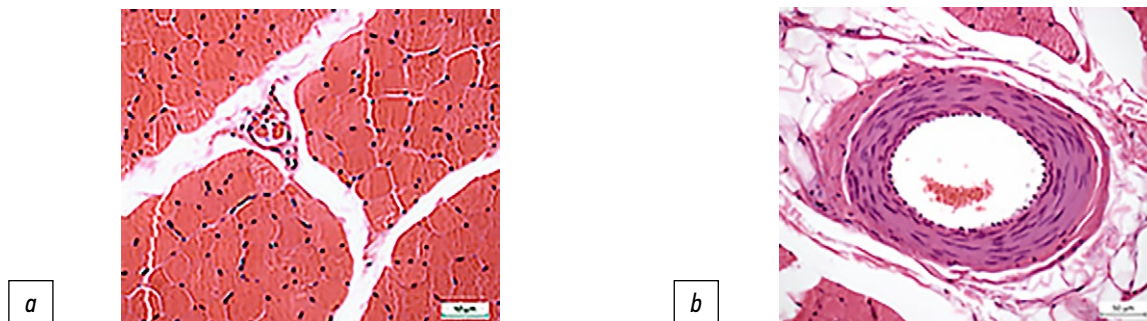


**Fig. 2.** Histostructure of *m. psoas minor* (a) and *m. sacrocaudalis (coccygeus) dorsalis lateralis* (b) in control: polygonal fiber profiles, minimum endomysium; a — neuromuscular spindle; (b) vessel in perimysium without signs of pathology. Fragments of paraffin sections, stained with hematoxylin-eosin; magnification  $\times 400$ .

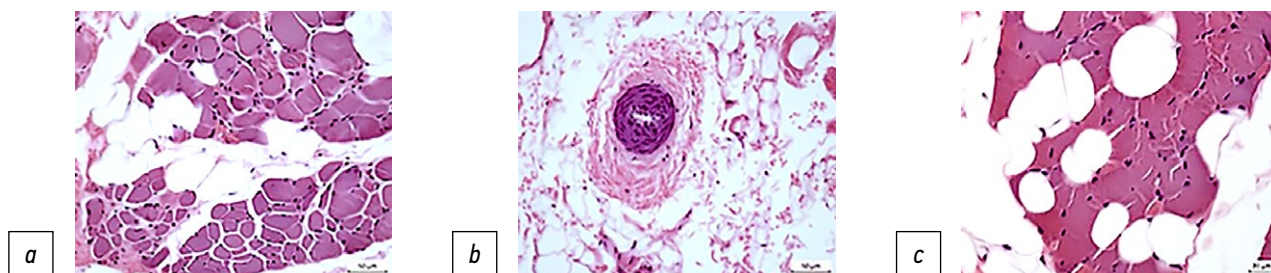


**Fig. 3.** Histostructure of the *psoas minor* (a, b) and the sacro-caudal (coccygeal) dorsal lateral muscle (c) after 6 months of the experiment: a, c — variability in the size of myosymplasts, endomysial fibrosis, adipocytes in bundles of muscle fibers; b — arterial vessel with severe fibrosis of the adventitial and middle membranes, impaired circular orientation of the smooth muscle cells, obliteration of the lumen. Fragments of paraffin sections; hematoxylin-eosin stain; magnification  $\times 400$ .

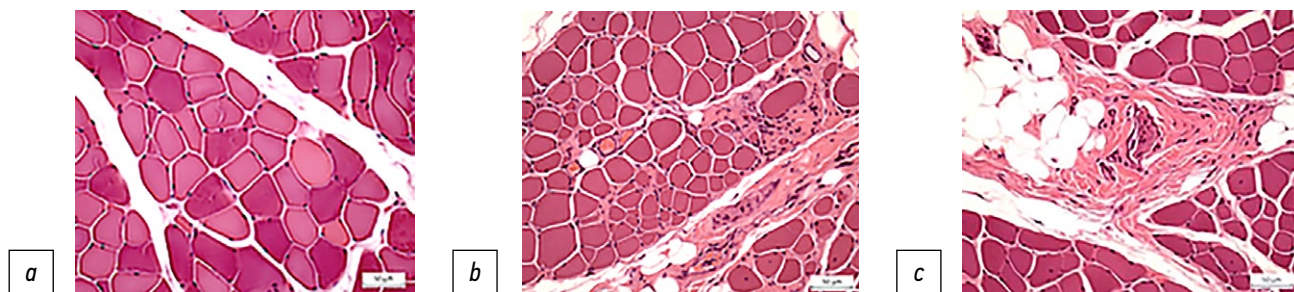


**Fig. 4.** Histostructure of *m. psoas minor* (a) and *m. sacrocaudalis (coccygeus) dorsalis lateralis* (b, c) after 12 months of the experiment: a — polygonal profiles of myosymplasts, minimum endomysium; b — variability in muscle fiber diameters, internal nuclei, an area of significant fibrosis of the interstitial tissue (on the right); c — a bundle of muscle fibers replaced by adipocytes; to the right, an area of fibrosis. Fragments of paraffin sections, stained with hematoxylin-eosin, magnification  $\times 400$ .

After 18 months, the histostructure of the studied muscles was characterized by a significant variety of visual fields. Thus, myosimplasts of different diameters and profiles were characteristic of small lumbar muscle and small groups of adipocytes replacing fibers in muscle bundles, fibrotic bundles of muscle fibers with angular small myocytes (Fig. 5a, below), and neuromuscular spindles of both normal structure and enlarged connective tissue capsules were present (Fig. 5b). In sacrocaudal (coccygeal) dorsal lateral muscles, fragments with polygonal fiber profiles and prominent endomysial fibrosis (Fig. 5c) were interspersed with adipocyte fields and fiber bundles, where myosimplasts in the ischemic state were visualized, which turned blue in Masson staining (Fig. 5d).

According to stereometry, the endomysial volume density increased in small lumbar and sacrocaudal

(coccygeal) dorsal lateral muscles after 6 months of the experiment, which was 150% ( $p < 0.05$ ) and 240% of the control value, respectively (Table 1). Furthermore, the proportion of myosimplastic volume decreased up to 95% of normal in the small lumbar muscle and up to 83% in the sacrocaudal muscle. The nuclear components of both muscles were 70% and 76% of normal, respectively ( $p < 0.05$ ). The volume densities of microvessels in the studied muscles were 83% and 121% of normal, respectively ( $p < 0.05$ ). The vascularization index in the lumbar muscle did not change, while accounting for 78% of normal in the second muscle. The rate of fat infiltration of the small lumbar muscle was 394% and that of the sacrocaudal muscle was 629% of the corresponding parameter in the control (Table 2).

After 12 months, the endomysial volumes in the small lumbar muscle and sacrocaudal dorsal lateral muscle

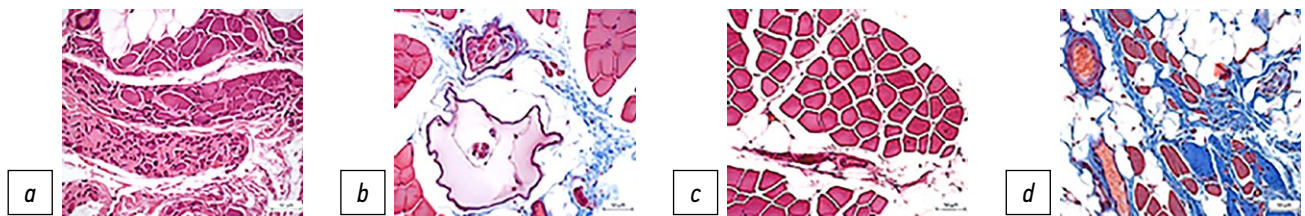


**Fig. 5.** Histostructure of the psoas minor (a, b) and *m. sacrocaudalis dorsalis lateralis* (c, d) after 18 months of the experiment: a — myocytes of various profiles and diameters, a group of adipocytes in the muscle bundle (top), a fragment of fibrosis with residual angular muscle fibers (bottom); b — neuromuscular spindles of normal structure and with an enlarged connective tissue capsular; c — polygonal fiber profiles, endomysial fibrosis; d — adipocytes that replaced part of the muscle fibers in the bundle, ischemic fibers are colored blue, fields of adipocytes. Fragments of paraffin sections, stained with hematoxylin-eosin, according to Masson (d); magnification  $\times 400$ .

**Table 1.** Data of the stereological analysis of the small lumbar (*m. psoas minor*) and sacrocaudal (coccygeal) dorsal lateral muscles (*m. sacrocaudalis (coccygeus) dorsalis lateralis*) of dogs

Parameters ( $\text{mm}^3/\text{mm}^3$ )	<i>M. psoas minor</i>				<i>M. sacrocaudalis (coccygeus) dorsalis lateralis</i>			
	6 months	12 months	18 months	Control	6 months	12 months	18 months	Control
$V_{\text{vmf}}$	0,7971* $\pm 0,0108$	0,7315* $\pm 0,0091$	0,7901* $\pm 0,009$	0,8299 $\pm 0,0042$	0,6975* $\pm 0,0166$	0,7001* $\pm 0,0107$	0,7181* $\pm 0,0118$	0,8439 $\pm 0,007$
$V_{\text{vmv}}$	0,0232* $\pm 0,003$	0,0283 $\pm 0,0034$	0,0175* $\pm 0,0043$	0,0281 $\pm 0,0025$	0,0272* $\pm 0,0038$	0,0251 $\pm 0,0027$	0,0216 $\pm 0,0034$	0,0225 $\pm 0,0028$
$V_{\text{vend}}$	0,1539* $\pm 0,0096$	0,2181* $\pm 0,0077$	0,1697* $\pm 0,0076$	0,1057 $\pm 0,0038$	0,2428* $\pm 0,0122$	0,2480* $\pm 0,0096$	0,2397* $\pm 0,0115$	0,1023 $\pm 0,0055$
$V_{\text{vn}}$	0,0238* $\pm 0,0029$	0,0216* $\pm 0,0027$	0,0195* $\pm 0,0046$	0,0347 $\pm 0,0026$	0,0238* $\pm 0,0029$	0,0216* $\pm 0,0027$	0,0195* $\pm 0,0046$	0,0312 $\pm 0,0032$
$I_{\text{vasc}}$	0,7872	0,9408	0,9043	0,7877	0,7431	0,9714	1,0925	0,9575

Note. \*Differences are significant for the experimental groups and control,  $p < 0.05$ .

were 206% and 243% of these parameters in the control, respectively ( $p < 0.05$ ). The volume densities of muscle fibers, microvessels, nuclear component, and vascularization index in the small lumbar and sacrococaudal muscles were 98% and 83%, 101% and 112%, 62% and 69%, and 119% and 101% of normal, respectively. The degree of fatty infiltration decreased relative to the previous period, amounting to 227% in the small lumbar muscle and 327% in the sacrococaudal (coccygeal) dorsal lateral muscle relative to the value of this parameter in the control group.

At month 18 of the experiment, the volume density of myosin, proportion of nuclear component, relative microvascular volume, and vascularization index in the small lumbar and sacrococaudal dorsal lateral muscles were 95% and 85% ( $p < 0.05$ ), 56% and 62% ( $p < 0.05$ ), 62% and 96% ( $p < 0.05$ ) of normal, respectively, and 115% and 114% of the parameter values in the control. The degree of sclerotization

of the small lumbar muscle decreased relative to the previous period, reaching 161% of the control and did not change in the sacrococaudal (coccygeal) dorsal lateral muscle, still accounting for 240% of the control value ( $p < 0.05$ ). The index of fat infiltration in the small lumbar muscle increased relative to the previous period by up to 339%, whereas decreasing insignificantly in the sacrococaudal dorsal lateral muscle, accounting for 310% of the parameter control values (Table 2).

The results of the biochemical study in the main group revealed a significant increase in the concentration of the C-reactive protein in the blood serum from days 14 to 30 after surgery (Table 3). On day 14, the level of total serum protein statistically significantly decreased, along with an increase in the activity of all enzymes (increase in CPK was over two-fold compared with the initial values).

**Table 2.** Fat infiltration of the small lumbar (*m. psoas minor*) and sacrococaudal (coccygeal) dorsal lateral muscles (*m. sacrocaudalis (coccygeus) dorsalis lateralis*) of dogs

Duration of the experiment	6 months	12 months	18 months	Control
<i>M. psoas minor</i>				
Proportion of adipocytes, %	28,0	16,1	24,1	7,1
<i>M. sacrocaudalis (coccygeus) dorsalis lateralis</i>				
Proportion of adipocytes, %	32,7	17,0	16,1	5,2

**Table 3.** Dynamics of changes in the biochemical parameters of blood serum during the experiment, median (1st; 3rd quartile)

24 h after surgery	Total protein, g/L	C-reactive protein, mg/L	Creatine phosphokinase, U/L	ALT, U/L	AST, U/L
0	68 (66; 71)	0	100 (78; 114)	32 (31; 40)	26 (21; 26)
14	64 (62; 66)*	2,3 (0,6; 4,0)*	215 (201; 234)*	47 (43; 56)*	34 (31; 39)*
30	69 (66; 71)	1,9 (0,2; 5,3)*	88 (86; 125)	29 (28; 35)	27 (24; 32)
60	65 (64; 67)	0	92 (81; 142)	27 (25; 33)	30 (23; 37)
90	66 (64; 68)	0	94 (87; 107)	29 (25; 33)	23 (19; 27)
180	67 (65; 68)	0	97 (93; 105)	33 (27; 36)	26 (20; 38)
360	65 (64; 68)	0	99 (89; 104)	33 (32; 43)	30 (25; 37)
540	70 (69; 70)	0	94 (84; 97)	33 (28; 43)	31 (23; 38)

Note. \* Significant differences with preoperative values at  $p < 0.05$ .

## DISCUSSION

Surgical interventions with lateral interbody fusion and posterior SIJ arthrodesis negatively affect both the small lumbar and sacrocaudal (coccygeal) dorsal lateral muscles, which is manifested both in the early postoperative period (significant increase in the activity of CPK, a marker of skeletal muscle damage) and during the experiment. This is evidenced by the variations in myosymplastic diameters, smoothing of polygonality of profiles, fibrosis of endomysial and perimysial connective tissue, sclerotization of arterial vessel tunics, lumen obliteration, and mass fatty degeneration of muscle fibers in the bundles. Activated nuclei along with variations in muscle fiber diameters indicate the structural adaptation of the muscle tissue to the surgical intervention. After 12 months, the volume density of the nuclei decreased simultaneously with a decrease in the volume fraction of myosymplasts. The decrease in the proportion of the nuclear component in the later period of the experiment may be due to the increasing age and restricted mobility of the experimental animals resulting from being held in a vivarium [21, 22]. Fibrosis of the small lumbar muscle was 1.5-fold, 2-fold, and 1.6-fold higher after 6, 12, and 18 months of the experiment, respectively, compared with the control. In the sacrocaudal (coccygeal) dorsal lateral muscle, this parameter did not change in all study periods and was 2.4-fold higher than that in the control. The degrees of fat involution of the small lumbar and sacrocaudal dorsal lateral muscles after 6, 12, and 18 months of the experiment were 3.9-fold and 6.3-fold, 2.3-fold and 3.3-fold, and 3.4-fold and 3.1-fold higher, respectively, than normal parameters. The sacrocaudal dorsal lateral muscle showed more pronounced changes during the experiment in both the degree of fibrosis and level of fat involution, particularly in the early stages of the experiment.

Clinical studies present data on the reduction of myosymplastic volume density, sclerotization, and fatty infiltration of the studied muscles under combined surgical treatment. Thus, paraspinal muscles showed different patterns of degeneration in lumbar spine diseases. A direct correlation was found between the severity of degenerative processes in the spinal column and the morphology of the back muscles [23]. Reduced paravertebral muscle volume correlated with kyphotic deformity in ankylosing spondylitis [24]. The volume of these muscles affects the consolidation rate, functional activity, and complication rates after surgery [16]. Fat involution is one of the leading

prognostic factors for the outcomes of surgical interventions, that is, the lower the degree of fat infiltration, the lower the pain syndrome and the percentage of postoperative functional decline [17]. In addition, fatty dystrophy of the back muscles is closely related to the mineral density of the spinal bone tissue [25–27]. Osteoporosis and paraspinal degeneration are frequently combined, which should be considered in patients with low bone mass before surgical intervention [14].

In clinical practice, a complex of physiotherapeutic methods including electrical stimulation of the back muscles, calcium electrophoresis, massage, paraffin therapy, and therapeutic exercise are employed to reduce the incidence of paravertebral muscle complications postoperatively [28]. This improves the muscle motor function and consequently the quality of life of patients.

In this study, the animals were kept in a confined space with no access to active physical activity for the entire experiment, which negatively affected the recovery processes in the muscle tissue and influenced the findings to some extent.

## CONCLUSIONS

Morphological analysis of the paravertebral muscles in the simultaneous simulation of lateral interbody fusion and posterior SIJ arthrodesis revealed pathohistological changes in both muscles such as increased variations of myosymplastic diameters, loss of the polygonality of their profiles, massive fatty degeneration of fibers, endomysial and perimysial fibrosis, sclerotization, and lumen obliteration of the vessels' tunics. After the experiment, the degree of sclerotization of the small lumbar muscle and sacrocaudal dorsal lateral muscle was 161% and 240%, respectively, of the control parameter values, and the rates of fat infiltration of muscles were 339% and 310% of normal, respectively. The sacrocaudal (coccygeal) dorsal lateral muscle went through more pronounced changes in both the degree of fibrosis and level of fat involution, particularly in the early stages of the experiment.

Considering that patients already have dystrophic processes in paravertebral muscles in degenerative spinal diseases at the time of referral to a neurosurgeon [17], surgical interventions should seek to minimize the mechanical effect on the back muscles and use techniques to stimulate muscle function postoperatively [28]. This will reduce fibrogenesis and fat involution in the muscles, improve functional activity, and provide an overall shorter rehabilitation period for the patients.



## ADDITIONAL INFO / ДОПОЛНИТЕЛЬНАЯ ИНФОРМАЦИЯ

**Author contribution.** Thereby, all authors made a substantial contribution to the conception of the work, drafting and revising the work, final approval of the version to be published and agree to be accountable for all aspects of the work.

**Вклад авторов:** Все авторы подтверждают соответствие своего авторства международным критериям ICMJE (все авторы внесли существенный вклад в разработку концепции и подготовку статьи, прочли и одобрили финальную версию перед публикацией).

## REFERENCES

1. Patel K, Tajsic T, Budohoski KP, et al. Simultaneous navigated cervico-thoracic and thoraco-lumbar fixation. *Eur Spine J.* 2018;27(3):318–322. doi: 10.1007/s00586-017-5233-1
2. Bari MM, Islam S, Shetu NH, Rahman M. Orthopedic control of injuries in polytrauma. *Genij Ortopedii.* 2017;23(3):351–353. doi: 10.18019/1028-4427-2017-23-3-351-35
3. Wang HW, Hu YC, Wu ZY, et al. One approach anterior decompression and fixation with posterior unilateral pedicle screw fixation for thoracolumbar osteoporotic vertebral compression fractures. *Orthop Surg.* 2021;13(3):908–919. doi: 10.1111/os.12947
4. Byvaltsev VA, Kalinin AA, Ryabykh SO, et al. Simultaneous surgical interventions in spinal neurosurgery: a systematic review. *Genij Orthopedii.* 2020;26(2):275–281. (In Russ). doi: 10.18019/1028-4427-2020-26-2-275-281
5. Li Y, Du Y, Ji A, et al. The Clinical Effect of Manual Reduction Combined with Internal Fixation Through Wiltse Paraspinal Approach in the Treatment of Thoracolumbar Fracture. *Orthop Surg.* 2021;13(8):2206–2215. doi: 10.1111/os.13090
6. Moulin B, Tselikas L, Gravel G, et al. Safety and Efficacy of Multilevel Thoracolumbar Vertebroplasty in the Simultaneous Treatment of Six or More Pathologic Compression Fractures. *J Vasc Interv Radiol.* 2020;31(10):1683–1689.e1. doi: 10.1016/j.jvir.2020.03.011
7. Klimov VS, Vasilenko II, Evsyukov AV, et al. The use of LLIF technology in adult patients with degenerative scoliosis: retrospective cohort analysis and literature review. *Genij Ortopedii.* 2018;24(3):393–403. (In Russ). doi: 10.18019/1028-4427-2018-24-3-393-403
8. Lorio M, Kube R, Araghi A. International Society for the Advancement of Spine Surgery Policy 2020 Update—Minimally Invasive Surgical Sacroiliac Joint Fusion (for Chronic Sacroiliac Joint Pain): Coverage Indications, Limitations, and Medical Necessity. *Int J Spine Surg.* 2020;14(6):860–895. doi: 10.14444/7156
9. Ladd B, Polly Jr D. Pelvic Fixation Using S2AI and Triangular Titanium Implants (Bedrock Technique). *World Neurosurg.* 2021;154:2. doi: 10.1016/j.wneu.2021.07.027
10. Panico M, Chande RD, Lindsey DP et al. Innovative sacropelvic fixation using iliac screws and triangular titanium implants. *Eur Spine J.* 2021;30(12):3763–3770. doi: 10.1007/s00586-021-07006-9
11. Rainov NG, Schneiderhan R, Heidecke V. Triangular titanium implants for sacroiliac joint fusion. *Eur Spine J.* 2019;28(4):727–734. doi: 10.1007/s00586-018-5860-1
12. Dale M, Evans J, Carter K, et al. iFuse Implant System for Treating Chronic Sacroiliac Joint Pain: A NICE Medical Technology Guidance. *Appl Health Econ Health Policy.* 2020;18(3):363–373. doi: 10.1007/s40258-019-00539-7
13. Novák V, Wanek T, Hrabálek L, Stejskal P. [Minimally Invasive Sacroiliac Joint Stabilization]. *Acta Chir Orthop Traumatol Cech.* 2021;88(1):35–38.
14. Han G, Zou D, Liu Z, et al. Paraspinal muscle characteristics on MRI in degenerative lumbar spine with normal bone density, osteopenia and osteoporosis: a case-control study. *BMC Musculoskelet Disord.* 2022;23(1):73. doi: 10.1186/s12891-022-05036-y
15. He K, Head J, Mouchtouris N, et al. The Implications of Paraspinal Muscle Atrophy in Low Back Pain, Thoracolumbar Pathology, and Clinical Outcomes After Spine Surgery: A Review of the Literature. *Global Spine J.* 2020;10(5):657–666. doi: 10.1177/2192568219879087
16. Khan AB, Weiss EH, Khan AW, et al. Back Muscle Morphometry: Effects on Outcomes of Spine Surgery. *World Neurosurg.* 2017;103:174–179. doi: 10.1016/j.wneu.2017.03.097
17. Jermy JE, Copley PC, Poon MTC, Demetriades AK. Does pre-operative multifidus morphology on MRI predict clinical outcomes in adults following surgical treatment for degenerative lumbar spine disease? A systematic review. *Eur Spine J.* 2020;29(6):1318–1327. doi: 10.1007/s00586-020-06423-6
18. Stevens S, Agten A, Timmermans A, Vandenabeele F. Unilateral changes of the multifidus in persons with lumbar disc herniation: a systematic review and meta-analysis. *Spine J.* 2020;20(10):1573–1585. doi: 10.1016/j.spinee.2020.04.007

19. Filimonova GN, Dyuryagina OV, Antonov NI, Ryabykh SO. Characteristics of the psoas minor in modeling lateral interbody fusion of the lumbar spine. *N.N. Priorov Journal of Traumatology and Orthopedics*. 2022;29(1):47–56. (In Russ). doi: 10.17816/vto90775
20. Gajdyshv IP. Modelirovanie stohasticheskikh i determinirovannykh sistem: Rukovodstvo pol'zovatelya programmy AtteStat. Kurgan, 2015. 484 p. Available from: [http://xn--80aab2abao2a1acibc.xn--p1ai/files/AtteStat\\_Manual\\_15.pdf](http://xn--80aab2abao2a1acibc.xn--p1ai/files/AtteStat_Manual_15.pdf). Accessed: 14.03.2023. (In Russ).
21. Chen W, Datzkiw D, Rudnicki MA. Satellite cells in ageing: use it or lose it. *Open Biol*. 2020;10(5):200048. doi: 10.1098/rsob.200048
22. Giza S, Mojica-Santiago JA, Parafati M, et al. Microphysiological system for studying contractile differences in young, active, and old, sedentary adult derived skeletal muscle cells. *Aging Cell*. 2022;21(7):e13650. doi: 10.1111/acer.13650
23. Ding JZ, Kong C, Li XY, et al. Different degeneration patterns of paraspinal muscles in degenerative lumbar diseases: a MRI analysis of 154 patients. *Eur Spine J*. 2022;31(3):764–773. doi: 10.1007/s00586-021-07053-2
24. Bok DH, Kim J, Kim TH. Comparison of MRI-defined back muscles volume between patients with ankylosing spondylitis and control patients with chronic back pain: age and spinopelvic alignment matched study. *Eur Spine J*. 2017;26(2):528–537. doi:10.1007/s00586-016-4889-2
25. Yang Q, Yan D, Wang L, et al. Muscle fat infiltration but not muscle cross-sectional area is independently associated with bone mineral density at the lumbar spine. *Br J Radiol*. 2022;95(1134):20210371. doi: 10.1259/bjr.20210371
26. Li X, Xie Y, Lu R, et al. Relationship between osteoporosis with fatty infiltration of paraspinal muscles based on QCT examination. *J Bone Miner Metab*. 2022;40(3):518–527. doi: 10.1007/s00774-022-01311-z
27. Zhao Y, Huang M, Serrano-Sosa M, et al. Fatty infiltration of paraspinal muscles is associated with bone mineral density of the lumbar spine. *Arch Osteoporos*. 2019;14(1):99. doi: 10.1007/s11657-019-0639-5
28. Koichubekov AA. The integrated approach to restorative treatment of patients with degenerative diseases of the lumbar spine after anterior spondylodesis. *Vestnik Kyrgyzsko-Rossiyskogo Slavânskogo Universiteta*. 2018;18(2):59–63. (In Russ).

## СПИСОК ЛИТЕРАТУРЫ

- Patel K., Tajsic T., Budohoski K.P., et al. Simultaneous navigated cervico-thoracic and thoraco-lumbar fixation // *Eur Spine J*. 2018. Vol. 27, N 3. P. 318–322. doi: 10.1007/s00586-017-5233-1
- Bari M.M., Islam S., Shetu N.H, Rahman M. Ортопедический контроль повреждений при политравме // *Гений ортопедии*. 2017. Т. 23, № 3. С. 351–353. doi: 10.18019/1028-4427-2017-23-3-351-353
- Wang H.W., Hu Y.C., Wu Z.Y., et al. One approach anterior decompression and fixation with posterior unilateral pedicle screw fixation for thoracolumbar osteoporotic vertebral compression fractures // *Orthop Surg*. 2021. Vol. 13, N 3. P. 908–919. doi: 10.1111/os.12947
- Бывальцев В.А., Калинин А.А., Рябых С.О. и др. Симультаные хирургические вмешательства в спинальной нейрохирургии: систематический обзор // *Гений ортопедии*. 2020. Т. 26, № 2. С. 275–281. doi: 10.18019/1028-4427-2020-26-2-275-281
- Li Y., Du Y., Ji A., et al. The Clinical Effect of Manual Reduction Combined with Internal Fixation Through Wiltse Paraspinal Approach in the Treatment of Thoracolumbar Fracture // *Orthop Surg*. 2021. Vol. 13, N 8. P. 2206–2215. doi: 10.1111/os.13090
- Moulin B., Tselikas L., Gravel G., et al. Safety and Efficacy of Multilevel Thoracolumbar Vertebroplasty in the Simultaneous Treatment of Six or More Pathologic Compression Fractures // *J Vasc Interv Radiol*. 2020. Vol. 31, N 10. P. 1683–1689. doi: 10.1016/j.jvir.2020.03.011
- Климов В.С., Василенко И.И., Евсюков А.В., и др. Применение технологии LLIF у пациентов с дегенеративным сколиозом поясничного отдела позвоночника: анализ ретроспективной когорты и обзор литературы // *Гений ортопедии*. Т. 24, № 3. С. 393–403. doi: 10.18019/1028-4427-2018-24-3-393-403
- Lorio M., Kube R., Araghi A. International Society for the Advancement of Spine Surgery Policy 2020 Update-Minimally Invasive Surgical Sacroiliac Joint Fusion (for Chronic Sacroiliac Joint Pain): Coverage Indications, Limitations, and Medical Necessity // *Int J Spine Surg*. 2020. Vol. 14, N 6. P. 860–895. doi: 10.14444/7156
- Ladd B., Polly Jr D. Pelvic Fixation Using S2AI and Triangular Titanium Implants (Bedrock Technique) // *World Neurosurg*. 2021. Vol. 154. P. 2. doi: 10.1016/j.wneu.2021.07.027
- Panico M., Chande R.D., Lindsey D.P., et al. Innovative sacropelvic fixation using iliac screws and triangular titanium implants // *Eur Spine J*. 2021. Vol. 30, N 12. P. 3763–3770. doi: 10.1007/s00586-021-07006-9
- Rainov N.G., Schneiderhan R., Heidecke V. Triangular titanium implants for sacroiliac joint fusion // *Eur Spine J*. 2019. Vol. 28, N 4, P. 727–734. doi: 10.1007/s00586-018-5860-1
- Dale M., Evans J., Carter K., et al. iFuse Implant System for Treating Chronic Sacroiliac Joint Pain: A NICE Medical Technology Guidance. *Appl Health Econ Health Policy* // 2020. Vol. 18, N 3. P. 363–373. doi: 10.1007/s40258-019-00539-7

13. Novák V., Wanek T., Hrabálek L., Stejskal P. [Minimally Invasive Sacroiliac Joint Stabilization] // *Acta Chir Orthop Traumatol Cech*. 2021. Vol. 88, N 1. P. 35–38.
14. Han G., Zou D., Liu Z., et al. Paraspinal muscle characteristics on MRI in degenerative lumbar spine with normal bone density, osteopenia and osteoporosis: a case-control study // *BMC Musculoskelet Disord*. 2022. Vol. 23, N 1. P. 73. doi: 10.1186/s12891-022-05036-y
15. He K., Head J., Mouchtouris N., et al. The Implications of Paraspinal Muscle Atrophy in Low Back Pain, Thoracolumbar Pathology, and Clinical Outcomes After Spine Surgery: A Review of the Literature // *Global Spine J*. 2020. Vol. 10, N 5. P. 657–666. doi: 10.1177/2192568219879087
16. Khan A.B., Weiss E.H., Khan A.W., et al. Back Muscle Morphometry: Effects on Outcomes of Spine Surgery // *World Neurosurg*. 2017. Vol. 103. P. 174–179. doi: 10.1016/j.wneu.2017.03.097
17. Jermy J.E., Copley P.C., Poon M.T.C., Demetriades A.K. Does pre-operative multifidus morphology on MRI predict clinical outcomes in adults following surgical treatment for degenerative lumbar spine disease? A systematic review // *Eur Spine J*. 2020. Vol. 29, N 6. P. 1318–1327. doi: 10.1007/s00586-020-06423-6
18. Stevens S., Agten A., Timmermans A., Vandenabeele F. Unilateral changes of the multifidus in persons with lumbar disc herniation: a systematic review and meta-analysis. *Spine J*. 2020. Vol. 20, N 10. P. 1573–1585. doi: 10.1016/j.spinee.2020.04.007
19. Филимонова Г.Н., Дюрягина О.В., Антонов Н.И., Рябых С.О. Характеристика малой поясничной мышцы при моделировании бокового межтелового спондилодеза поясничного отдела позвоночника // *Вестник травматологии и ортопедии им. Н.Н. Приорова*. 2022. Т. 29, № 1. С. 47–56. doi: 10.17816/vto90775
20. Гайдышев И.П. Моделирование стохастических и детерминированных систем: Руководство пользователя программы AtteStat. Курган, 2015. 484 с. Режим доступа: [http://xn--80aab2abao2a1acibc.xn--p1ai/files/AtteStat\\_Manual\\_15.pdf](http://xn--80aab2abao2a1acibc.xn--p1ai/files/AtteStat_Manual_15.pdf). Дата обращения: 14.03.2023.
21. Chen W., Datzkiw D., Rudnicki M.A. Satellite cells in ageing: use it or lose it. *Open Biol* // 2020. Vol. 10, N 5. P. 200048. doi: 10.1098/rsob.200048
22. Giza S., Mojica-Santiago J.A., Parafati M., et al. Microphysiological system for studying contractile differences in young, active, and old, sedentary adult derived skeletal muscle cells // *Aging Cell*. 2022. Vol. 21, N 7. P. e13650. doi: 10.1111/ace1.13650
23. Ding J.Z., Kong C., Li X.Y., et al. Different degeneration patterns of paraspinal muscles in degenerative lumbar diseases: a MRI analysis of 154 patients // *Eur Spine J*. 2022. Vol. 31, N 3. P. 764–773. doi: 10.1007/s00586-021-07053-2
24. Bok D.H., Kim J., Kim T.H. Comparison of MRI-defined back muscles volume between patients with ankylosing spondylitis and control patients with chronic back pain: age and spinopelvic alignment matched study // *Eur Spine J*. 2017. Vol. 26, N 2. P. 528–537. doi:10.1007/s00586-016-4889-2
25. Yang Q., Yan D., Wang L., et al. Muscle fat infiltration but not muscle cross-sectional area is independently associated with bone mineral density at the lumbar spine // *Br J Radiol*. 2022. Vol. 95, N 1134. P. 20210371. doi: 10.1259/bjr.20210371
26. Li X., Xie Y., Lu R. et al. Relationship between osteoporosis with fatty infiltration of paraspinal muscles based on QCT examination // *J Bone Miner Metab*. 2022. Vol. 40, N 3. P. 518–527. doi: 10.1007/s00774-022-01311-z
27. Zhao Y., Huang M., Serrano-Sosa M., et al. Fatty infiltration of paraspinal muscles is associated with bone mineral density of the lumbar spine // *Arch Osteoporos*. 2019. Vol. 14, N 1. P. 99. doi: 10.1007/s11657-019-0639-5
28. Койчубеков А.А. Комплексный подход к восстановительному лечению больных с дегенеративными заболеваниями поясничного отдела позвоночника после переднего спондилодеза // *Вестник Кыргызско-Российского Славянского университета*. 2018. Т. 18, № 2. С. 59–63.

## AUTHORS INFO

\*Galina N. Filimonova, Cand. Sci. (Biol.),  
Senior Research Associate;  
address: 6 M. Ulyanova str., 640014 Kurgan, Russia;  
ORCID: <https://orcid.org/0000-0003-0683-9758>;  
eLibrary SPIN: 5873-2280;  
e-mail: galnik.kurgan@yandex.ru

Olga V. Diuriagina, Cand. Sci. (Vet.),  
Head of the Experimental Laboratory;  
ORCID: <https://orcid.org/0000-0001-9974-2204>;  
eLibrary SPIN: 8301-1475;  
e-mail: diuriagina@mail.ru

## ОБ АВТОРАХ

\*Филимонова Галина Николаевна, к.б.н.,  
старший научный сотрудник;  
адрес: Россия, 640014, Курган, ул. М. Ульяновой, д. 6;  
ORCID: <https://orcid.org/0000-0003-0683-9758>;  
eLibrary SPIN: 5873-2280;  
e-mail: galnik.kurgan@yandex.ru

Дюрягина Ольга Владимировна, к.в.н.,  
заведующая экспериментальной лабораторией;  
ORCID: <https://orcid.org/0000-0001-9974-2204>;  
eLibrary SPIN: 8301-1475;  
e-mail: diuriagina@mail.ru

**Nikolai I. Antonov**, Cand. Sci. (Biol.),  
Research Associate;  
ORCID: <https://orcid.org/0000-0002-8627-2749>;  
eLibrary SPIN: 3754-7508;  
e-mail: aniv-niko@mail.ru

**Maksim V. Stogov**, Dr. Sci. (Biol.), Assistant Professor,  
Head of the Department of Preclinical and Laboratory Research;  
ORCID: <https://orcid.org/0000-0001-8516-8571>;  
eLibrary SPIN: 9345-8300;  
e-mail: Stogo\_off@list.ru

**Sergei O. Ryabikh**, MD, Dr. Sci. (Med.),  
Deputy Director for Projects, Education and Communication;  
ORCID: <https://orcid.org/0000-0002-8293-0521>;  
eLibrary SPIN: 6382-1107;  
e-mail: RyabikhSO@cito-priorov.ru

**Natalia V. Tushina**, Cand. Sci. (Biol.),  
Research Associate;  
ORCID: <https://orcid.org/0000-0002-1322-608X>;  
eLibrary SPIN: 7554-9130;  
e-mail: ntushina76@mail.ru

**Антонов Николай Иванович**, к.б.н.,  
научный сотрудник;  
ORCID: <https://orcid.org/0000-0002-8627-2749>;  
eLibrary SPIN: 3754-7508;  
e-mail: aniv-niko@mail.ru

**Стогов Максим Валерьевич**, д.б.н., доцент,  
руководитель отдела доклинических и лабораторных  
исследований;  
ORCID: <https://orcid.org/0000-0001-8516-8571>;  
eLibrary SPIN: 9345-8300;  
e-mail: Stogo\_off@list.ru

**Рябых Сергей Олегович**, д.м.н.,  
заместитель директора по проектам, образованию  
и коммуникации;  
ORCID: <https://orcid.org/0000-0002-8293-0521>;  
eLibrary SPIN: 6382-1107;  
e-mail: RyabikhSO@cito-priorov.ru

**Тушина Наталья Владимировна**, к.б.н.,  
научный сотрудник;  
ORCID: <https://orcid.org/0000-0002-1322-608X>;  
eLibrary SPIN: 7554-9130;  
e-mail: ntushina76@mail.ru

\* Corresponding author / Автор, ответственный за переписку